(12)

AD-A233 637

CUMENTATION PAGE

1b RESTRICTIVE MARKINGS

2a SECURITY CLASSIFICATION AUTHORITY

3 DISTRIBUTION AVAILABILITY OF REPORT
Approved for public release; distribution unlimited.

2b DECLASSIFICATION/DOWNGRADING SCHEDULE
Unclassified

4 PERFORMING ORGANIZATION REPORT NUMBER(S)
N00014-89-J-1237

5 MONITORING ORGANIZATION REPORT NUMBER(S)

6a NAME OF PERFORMING ORGANIZATION
Colorado State University

6b OFFICE SYMBOL (If applicable)

7a NAME OF MONITORING ORGANIZATION

6c ADDRESS (City, State, and ZIP Code)
Department of Chemistry
Fort Collins, CO 80523

7b ADDRESS (City, State, and ZIP Code)

8a NAME OF FUNDING/SPONSORING ORGANIZATION
Office of Naval Research

8b OFFICE SYMBOL (If applicable)

9 PROCUREMENT INSTRUMENT IDENTIFICATION NUMBER
N00014-89-J-1237

8c ADDRESS (City, State, and ZIP Code)
800 North Quincy Street
Arlington, VA 22217-5000

10 SOURCE OF FUNDING NUMBERS

PROGRAM ELEMENT NO	PROJECT NO	TASK NO	WORK UNIT ACCESSION NO

11 TITLE (Include Security Classification) Excited State Intermolecular Proton Transfer in Isolated Clusters: 1-Naphthol/Ammonia and Water

12 PERSONAL AUTHOR(S)
S. K. Kim, S. Li and E. R. Bernstein

13a TYPE OF REPORT	13b TIME COVERED	14 DATE OF REPORT (Year Month Day)	15 PAGE COUNT
Technical Report	FROM _____ TO _____	March 7, 1991	

16 SUPPLEMENTARY NOTATION

17 COSATI CODES		
FIELD	GROUP	SUB-GROUP

18 SUBJECT TERMS (Continue on reverse if necessary and identify by block number)
excited singlet state intermolecular proton transfer reaction, jet-cooled clusters, 1-naphthol/ammonia, mass resolved excitation, threshold photo-ionization, emission spectroscopy, water cluster systems, cluster geometry

19 ABSTRACT (Continue on reverse if necessary and identify by block number)

SEE ATTACHED ABSTRACT

DTIC ELECTE MAR 20 1991 S D D

20 DISTRIBUTION/AVAILABILITY OF ABSTRACT
☒ UNCLASSIFIED/UNLIMITED ☐ SAME AS RPT ☐ DTIC USERS

21 ABSTRACT SECURITY CLASSIFICATION
Unclassified

22a NAME OF RESPONSIBLE INDIVIDUAL
Elliot R. Bernstein

22b TELEPHONE (Include Area Code)
(303) 491-6347

22c OFFICE SYMBOL

DD Form 1473, JUN 86 Previous editions are obsolete

S/N 0102-LF-014-6603

91 3 19 0 0

OFFICE OF NAVAL RESEARCH
Contract N00014-89-J-1237
TECHNICAL REPORT #73

Excited State Intermolecular Proton Transfer in Isolated Clusters: 1-Naphthol/Ammonia and Water

S. K. Kim, S. Li, E. R. Bernstein

Submitted to the
JOURNAL OF CHEMICAL PHYSICS

Chemistry Department
Colorado State University
Fort Collins, CO

March 7, 1991

Accession For
NTIS CRA&I
DTIC TAB
Unannounced
Justification
By
Distribution /
Availability Codes
Dist | Avail and/or Special
A-1

Reproduction in whole or in part is permitted for any purpose of the United States Government.

This document has been approved for public release and sale; its distribution is unlimited.

ABSTRACT

The excited singlet state intermolecular proton transfer reaction in jet-cooled clusters of 1-naphthol/ammonia and water is investigated employing mass resolved excitation, threshold photo-ionization, and emission spectroscopy. The complete data set indicates that no proton transfer occurs for 1-naphthol$(NH_3)_{1,2}$ and $(H_2O)_n$, n = 1, ..., 20 clusters. Proton transfer occurs for (at least) one configuration of the 1-naphthol$(NH_3)_3$ cluster, as well as all 1-naphthol$(NH_3)_n$, n $\geq$ 4, clusters. The (at least) two configurations of 1-naphthol$(NH_3)_3$ clusters are distinguished by threshold photo-ionization studies. The 1-naphthol$(NH_3)_3$ cluster for which proton transfer is indicated has a threshold photo-ionization energy roughly 2000 cm^{-1} below the other 1-naphthol $(NH_3)_3$ cluster configurations. These results are employed to explain the previous discrepancy between static spectroscopic experiments and picosecond time resolved dynamic experiments concerning proton transfer in the 1-naphthol$(NH_3)_3$ cluster. Calculations of cluster geometry in 1-naphthol/ammonia and water cluster systems suggest some qualitative explanations of these observations.

I. INTRODUCTION

Proton transfer reactions are one of the elementary chemical reactions that play an important role in numerous chemical and biological processes. Photo-induced proton transfer reactions are also ubiquitous in chemistry and biology and offer the added advantage of ready access for kinetic and mechanistic studies.[1] Photo-induction allows the experimenter to initiate the reaction and thus the mechanistic sequence can be followed with time at a point of his choosing. One of the major issues for reactions of any sort, and elementary reactions (i.e., proton transfers and electron transfers) in particular, is the role of the solvent in the reaction mechanism and kinetics. One can study the role played by the solvent in such reactions by controlling its presence in the reacting system. This can be accomplished in a number of instances through the study of chemical reactions in small solute/solvent clusters of known size and often geometry, as generated in a supersonic expansion.[2] The clusters may then be accessed by optical and mass spectroscopy and the reaction studied as a function of many separate cluster parameters.

Almost all excited state proton transfer chemical reactions in large molecules or clusters that have been investigated are of the form

$$(AH)B_n \xrightarrow[h\nu]{} (AH)^*B_n \longrightarrow A^{*-}(HB_n)^+. \qquad (1)$$

In these cases the requirements for the excited state proton transfer reaction in the cluster are as follows: 1. the chromophore solute (AH) must be a good acid in the excited state (small pK_a in S_1) and a poor acid in the ground state (large pK_a in S_0) - the concomitant change in pK_a upon excitation can be estimated by a Förster cycle calculation;[3,4] 2. AH must have relatively high vapor pressure and a strong $S_1 \leftarrow S_0$ transition; and 3. the solvent (cluster) B_n must have large a proton affinity.

The number of systems of this nature thus far investigated by supersonic expansion optical/mass spectroscopy techniques has been relatively small: convincing evidence has been presented for 1-naphthol/ammonia[5-8] and piperidine[7,8]; 2-naphthol/ammonia[9];

phenol/ammonia[10,11] and ethylamine[12]; hydroxypyridine/pyridone/ammonia[13]; and an intramolecular proton transfer in 2,5-bis(2-benzoxazolyl)hydroquinone.[14] We will shortly publish our proton transfer findings for 2-substituted phenols (allyl, propenyl, propyl) clustered with ammonia and water.[15]

The general questions one hopes to answer with such studies of cold clusters are the following: 1. what is the mechanism for the excited state proton transfer; 2. will knowledge of this mechanism aid in the understanding of solution phase behavior; 3. what is the critical number of solvent molecules in the cluster for which the excited state proton transfer is induced; 4. what determines this critical number; and 5. how important is specific cluster and solvent geometry for the reaction?

Several recent studies[5-12] have placed emphasis on the critical cluster size (i.e., the number n of solvent molecules) for which intermolelcular proton transfer is induced. In general, a number of spectroscopic observations can be employed to suggest that proton transfer reactions have occurred in clusters. First, the excitation spectrum can be broad due to coupling of the S_1 state of the chromophore to the high density of product states and/or to a reduced lifetime for the unreacted cluster states. Second, red shifted emission can arise from the product state $A^{*-}(HB_n)^+$ in addition to or instead of the normal reactant $AH^*(B_n)$ emission. Third, a red shift in the ionization threshold is expected upon proton transfer in S_1 because the product $A^{*-}(HB_n)^+$ has stabilized separated charges and thus should ionize at lower energy. Fourth, dynamical behavior can be associated with any and all of these changes - it can be followed with time resolved spectroscopic techniques. Figure 1a represents the potential curves and electronic transitions that might give rise to such behavior assuming n = 3 is the critical cluster solvent size for the proton transfer reaction.

None of the above harbingers of proton transfer in clusters is without its own complications, however. Broadening of the excitation features can be caused by contributions from spectral congestion due to other clusters or the inhomogenous broadening from the clusters' own density of states. The emission spectra are of necessity always obtained without mass resolution and thus the exact value of critical cluster size cannot be obtained definitively based only

on emission studies. Threshold photo-ionization does yield mass information; but the red shift that occurs upon cluster size increase due to differential increased binding in the ionic cluster compared to the neutral cluster and changes in Franck-Condon factors for ionization can obscure the ionization changes associated with internal cluster charge separation (Figure 1b). Three photon ionization processes can also interfere with expected two photon trends.[16] Time resolved spectroscopy (emission and mass resolved) may be the ultimate tool for these determinations, but even this method of detection for proton transfer relies on a precise analysis of the steady state spectra. One is forced to conclude that only a combination of these many techniques will yield a reliable indication that proton transfer (chemical reaction) has occurred for a particular cluster in the S_1 excited electronic state.

Recently, picosecond pump/probe experiments employing mass selective detection were reported for jet-cooled 1-naphthol[8] and phenol[11] clustered with water and ammonia. The reported observations for water clusters are in agreement with the steady state results[6,17]: no proton transfer occurs even for $n > 20$. Agreement between static and dynamic measurements for 1-naphthol $(piperidine)_n$ clusters is also good: $n \geq 2$ induces the S_1 transfer of a proton.[8,9] Agreement on the critical size for excited state proton transfer in 1-naphthol/ammonia clusters and phenol/ammonia clusters is not good, however. Static spectra (emission) of 1-naphthol/ammonia clusters suggest transfer occurs at $n = 4$,[6] while dynamic results suggest $n = 3$ clusters[8] induce transfer. Static threshold ionization results for phenol/ammonia clusters suggest proton transfer in $n = 4$ clusters[10] while the dynamic results[11] lead to the conclusion that transfer occurs only at $n = 5$ phenol/ammonia clusters.

In this report we discuss and emphasize mass resolved excitation spectra and threshold photo-ionization data for 1-naphthol/ammonia and water clusters as a function cluster size (solvent number n). We find that not only does excited state (S_1) proton transfer depend on the number of solvent molecules present in the cluster, but it also apparently is a function of the cluster structure. One cluster of 1-naphthol$(NH_3)_3$ has a very low ionization energy threshold (equal to that of $n = 4$ clusters) and we suggest that this cluster, due to a particularly advantageous solvation structure,

induces excited state proton transfer while other n = 3 clusters do not. Excited state proton transfer apparently occurs for all 1-naphthol$(NH_3)_n$ clusters for $n \geq 4$. This conclusion rationalizes the static and dynamic data for the 1-naphthol/ammonia proton transfer system.[5-8] We attempt to understand these results in terms of trends in cluster structures calculated with a standard intermolecular potential energy function and an energy minimization algorithm.

II. EXPERIMENTAL PROCEDURES

One-color and two-color mass resolved excitation spectra of 1-naphthol and its clusters with water and ammonia are obtained in the usual manner.[18] The laser systems consist of Nd/YAG pumped dye lasers whose independently turnable outputs are doubled or mixed with residual 1.064 μm light to match the $S_1 \leftarrow S_0$ and $I \leftarrow S_1$ transitions of the appropriate clusters of interest.

1-naphthol is purchased from Aldrich Chemical Co. and placed in a heated pulsed nozzle at 65°C.

Intensity of the ionization laser is monitored and maintained between 300 and 1000 μJ/pulse. The energy of the $S_1 \leftarrow S_0$ excitation pulse is attenuated to approximately 2 μJ for 1-naphthol$(NH_3)_1$, 20 μJ for 1-naphthol$(NH_3)_2$ and $(H_2O)_1$, 50 μJ for 1-naphthol$(NH_3)_3$, and 150 μJ for 1-naphthol$(NH_3)_4$ cluster studies. Since the threshold is broad for these clusters, we simply take the wavelength at which photo-ionization current disappears for the threshold.

Dispersed emission is obtained by the use of UV cut-off filters (Hoya U34, U36, L38, L40) placed in front of the photo tube.

Calculations of cluster geometries are accomplished as we have previously reported.[13] Molecules (solute and solvent) are randomly placed in a box of chosen size and an energy minimization algorithm finds the lowest energy local geometry for the molecules. The calculations are repeated many times to find all the possible local energy minima on the potential surface.

The interaction energy between the molecules of the cluster for a given geometry is calculated based on a potential energy function containing coulomb, hydrogen bonding (when appropriate) and Lennard-Jones atom-atom terms.[19]

Geometries and point change distributions for both the solute and solvent are obtained from MOPAC 5/PM3 calculations[20] prior to the potential energy minimization.

III. RESULTS

A. Mass resolved Excitation Spectroscopy

The mass resolved excitation spectra of 1-naphthol and some of its clusters with ammonia and water are presented in Figure 2. The bare molecule electronic origin is located at 31,458 cm^{-1}. This feature has been suggested to arise from the anti-1-naphthol conformer[21-23] indicated in Scheme I. In our experiment the syn isomer has only negligible population (origin at

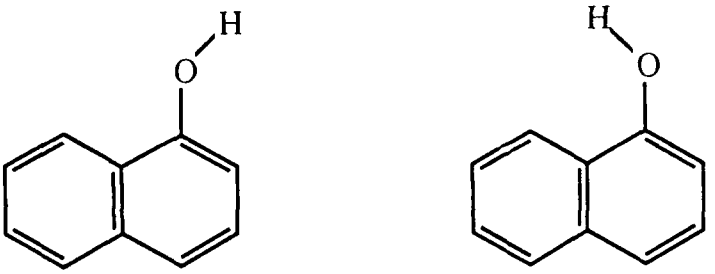

Anti Syn

1-Naphthol

31,182 cm^{-1}) and therefore no significant effort has been made to obtain its cluster spectra.

As the 1-naphthol/water clusters become larger, $1 \leq n \leq 7$, the spectra become broader with a few sharp features appearing above a broad background.[17]

The clusters of 1-naphthol with ammonia appear to have somewhat different mass resolved excitation spectra than those found with water (Figure 2). The 1-naphthol$(NH_3)_1$ cluster

apparently shows a single origin feature at 31,220 cm^{-1}. Multiple features are observed for the 1-naphthol$(NH_3)_2$ clusters probably due to both different cluster conformations and van der Waals mode intensity. Unlike the situation found for 1-naphthol$(H_2O)_n$, n = 2, 3, 4, ..., no fragmentation peaks are observed for the ammonia clusters with n = 1, 2, 3. The 1-naphthol$(NH_3)_{4, 5, ...}$ clusters have red shifted, featureless, broad spectra. These findings are in complete agreement with those of previous studies.[6]

As the clusters become larger, their spectra become generally more complex and broad. To distinguish the contributions to this spectral congestion (i.e., conformers and van der Waals modes of a single species), one can compare the 1-color and near threshold 2-color mass resolved excitation spectra of the various cluster masses. Such a comparison for 1-naphthol$(NH_3)_3$ is presented in Figure 3. The possibility that many of the sharp features in the 1-color spectrum of 1-naphthol$(NH_3)_3$ are due to fragmentation of higher order clusters can be eliminated because the $n \geq 4$ ammonia clusters do not evidence sharp features in any spectral region. Thus the fact that the 1- and 2-color spectra are so different for this cluster must be attributed to clusters of this mass but with different conformations and thus different ionization energies. At sufficiently low ionization energy (ν_{ion} ~ 26, 500 cm^{-1}) most of the sharp peaks in the mass resolved excitation spectrum of 1-naphthol$(NH_3)_3$ disappear and a "new feature" emerges at ca. 31,105 cm^{-1} which was previously obscured by more intense features from $(NH_3)_3$ clusters (of different geometry) with higher ionization energies. Figure 3 and additional ionization data suggest that the spectral congestion is due to contributions from many (perhaps 5 or more) 1-naphthol$(NH_3)_3$ cluster conformations.

B. Threshold Photo-Ionization

Figure 4 shows the threshold photo-ionization intensities as a function of total ionization energy for 1-naphthol$(H_2O)_1$ and $(NH_3)_{1, 2, 3, 4}$. The threshold values or vertical ionization potentials are summarized in Table I. The threshold ionization potential values for the $(H_2O)_1$ and $(NH_3)_{1, 2}$ clusters are lower than the bare molecule value by approximately 3600, 5000, and 5100 cm^{-1}, respectively. The ionization potentials for 1-naphthol$(H_2O)_n$ (n = 1, 2, 3,

4) are quite close to one another and do not appear to vary systematically with n. The ionization threshold for 1-naphthol$(NH_3)_3$ clusters differs depending on the value of ionization excitation energy in the region of the origin transition ca. 31,040 to 31,120 cm^{-1}; that is, depending on the cluster conformer selected in the $S_1 \leftarrow S_0$ excitation. Conformers which absorb around 31,070, 31,090, and 31,100 cm^{-1} have ionization thresholds similar to that found for 1-naphthol$(NH_3)_{1,2}$ clusters. The ionization potential for the conformer absorbing near 31,050 cm^{-1} is about 200 cm^{-1} red shifted from these latter features. In contrast, the conformer of 1-naphthol$(NH_3)_3$ which has an $S_1 \leftarrow S_0$ absorption ca. 31,105 cm^{-1} has an ionization threshold some 1500 to 2000 cm^{-1} red shifted from the other conformers.

C. Dispersed Emission

Dispersed emission studies of 1-naphthol/water and ammonia clusters reveal a red shifted component ($\Delta\nu \sim 8000$ cm^{-1}) of the emission for 1-naphthol$(NH_3)_n$, $n \geq 4$,[6] but not $n = 3$. In this regard recall that dispersed emission is obtained without mass resolution and note the n = 3 and 4 spectra presented in Figure 2 for ammonia clusters. With these difficulties in mind, we have attempted to reproduce the reported dispersed emission data for 1-naphthol$(NH_3)_n$, n = 1, 2, 3, 4, clusters employing very low (0.002%) and controlled concentrations of NH_3 and UV filters placed in front on the phototube. A portion of the observed, generally weak, emission is presented in Figure 5. Figures 5a, b, c show fluorescence excitation spectra about the origin regions of 1-naphthol$(NH_3)_{2,3}$ clusters as observed through several cut off filters. With a UV34 filter (Figure 5a, see caption for transmission details - essentially transmits radiation of energy lower than 31,750 cm^{-1}, ≥ 320 nm) all the 1-naphthol$(NH_3)_{2,3}$ features can be observed. Note that the feature at ca. 31105 cm^{-1} should contain emission from both $(NH_3)_2$ and $(NH_3)_3$ clusters. With lower energy cut off filters (UV36 - 0% transmission $\leq$ 340 nm or $\geq$ 29,400 cm^{-1} and L38 - 0% transmission $\leq$ 350 nm or $\geq$ 28,500 cm^{-1}), the peak at ca. 31,105 cm^{-1} still persists suggesting that only red shifted emission is generated by the $(NH_3)_3$ cluster that absorbs at this energy. Note that this feature would not be detected with a monochromator at this concentration of NH_3 in the expansion (f/1 vs f/8 optics).

In contrast, red shifted emission is observed from excitation of the broad features corresponding to 1-naphthol$(NH_3)_n$, $n \geq 4$. This emission could mask other red shifted emission associated with the broad absorptions for 1-naphthol$(NH_3)_3$ clusters (see Figure 2).

D. Cluster Structure Calculations for 1-Naphthol$(NH_3)_n$ and $(NH_3)_n$

One of the strong implications that arises from the spectroscopic data presented in this section is that for clusters of a given n-value (size or mass), a number of different cluster conformation of solvent molecules with respect to the solute molecule, and, indeed, the other solvent molecules as well, can be identified. In particular, for 1-naphthol$(NH_3)_3$, the above data suggest that (at least) one cluster geometry supports proton transfer while others do not. Cluster geometry thus becomes an issue for the proton transfer reaction. Apparently, solvent cluster proton affinity is not the only determining factor for the reaction of eq. (1). Thus, most likely both the resulting anion and the proton require some degree of solvation for the reaction free energy to be favorable.

1. 1-Naphthol$(H_2O)_1$

Three geometries are found for the 1-naphthol$(H_2O)_1$ cluster as shown in Figure 6. The figure presents three different pieces of information concerning the cluster: structures, binding energy and the frequency with which the given structure is found. This latter information is in some sense the probability for the formation of this cluster in a random encounter between solute and solvent. Thus the structures of Figure 6a and 6b are difficult to form while that of 6c is easy because of the large acceptable "angle of approach" for this structure. Nonetheless, due to collisions in the jet, the lower energy (rarer) structures are most likely the ones that actually form. The most stable structure (Figure 6a) involves the naphtholic hydrogen hydrogen bonded to the water oxygen. This is probably the single cluster observed in our spectrum of 1-naphthol $(H_2O)_1$.

2. 1-Naphthol$(H_2O)_{2,3,4}$

Many stable structures are calculated for 1-naphthol $(H_2O)_2$: a few of the lowest energy of these are presented in Figure 7. For the most part, these structures involve water coordinated to the naphthol OH group and to the other water molecule present. Again these structures appear infrequently in the computer calculations but they probably dominate in the experiment due to collisional "activation" or collision induced barrier crossings on the potential surface of the forming clusters. Coordination to the π-system is much less energetically favorable (by roughly a factor of two). Similar trends are identified for 1-naphthol$(H_2O)_{3,4,}$ clusters (Figures 8 and 9). The waters all hydrogen bond together in the proximity of the solute OH group.

3. 1-Naphthol$(NH_3)_1$

The calculated geometries for ammonia clusters are quite different from those for water clusters. Figure 10 presents the 1-naphthol$(NH_3)_1$ cluster geometries. Here the lowest energy clusters show a mixture of NH_3 - *π–system coordination and hydrogen bonding* (ammoni - hydrogen to naphtholic oxygen). This is consistent with and emphasizes the commonly held notion that O-H hydrogen bonding is stronger than N-H hydrogen bonding.

4. 1-Naphthol$(NH_3)_{2,3,4}$

The trend for large ammonia clusters is also somewhat different from that found for the larger water clusters: hydrogen bonding is emphasized to a much smaller extent and NH_3 π-system interactions become dominant. Since the NH_3 - NH_3 interaction energy is smaller than the NH_3 - 1-naphthol interaction energy (~ 430 vs 1100 cm^{-1} for the potentials employed here) the ammonia molecules do not necessarily bond together, but rather occupy positions that distribute them about the 1-naphthol solute: that is, the ammonia molecules better solvate the 1-naphthol solute. The general interaction, as can be seen readily in Figures 11, 12 and 13 however, takes place with a bias toward the OH portion of the 1-naphthol.

IV. DISCUSSION

A. Threshold Photo-Ionization

The threshold photo-ionization spectra recorded in Figure 4 and summarized in Table I separate the 1-naphthol water and ammonia clusters into three groups: 1. 1-naphthol $(H_2O)_n$, n = 1, ..., 4 with ionization threshold ca. 59,000 ± 200 cm^{-1}; 2. 1-naphthol$(NH_3)_{1,2}$ and most of the 1-naphthol$(NH_3)_3$ conformers with ionization threshold ca. 57,500 ± 200 cm^{-1}; and 3. one of the 1-naphthol$(NH_3)_3$ conformers and all 1-naphthol$(NH_4)_n$, n ≥ 4, conformers with ionization thresholds ca. 56,000 cm^{-1}. The ionization threshold red shifts for the first two groups of clusters simply reflect the binding energy differences between the neutral ground state and the ion (ca. 2500 and 4000 cm^{-1}, respectively). By way of comparison, the ionization potentials for the clusters indole$(H_2O)_1$ and $(NH_3)_{1,2}$, for which no proton transfer has been characterized, are red shifted from the indole ionization potential by 3000, 4150 and 4550 cm^{-1}, respectively.[24]

In contrast, the large relative shift for the third grouping of clusters (ca. 6650 cm^{-1}) seems to suggest that proton transfer has occurred in these S_1 excited state systems. Perhaps the major advantage of threshold photo-ionization studies over the dispersed emission studies of proton transfer is that the ionization studies employ mass resolution. Each technique has limitations with regard to selectivity, sensitivity and interpretation, especially near the limits of the techniques (i.e., $(NH_3)_3$ vs. $(NH_3)_4$ clusters); however, the confluence of the three techniques, threshold ionization, dispersed emission, and time resolved, all yielding similar results is indeed compelling.

B. Comparison with Previous Results

All results for proton transfer in 1-naphthol$(NH_3)_n$, n ≥ 4, and 1-naphthol$(H_2O)_n$, n = 1, ... > 20, agree: proton transfer in S_1 occurs in the first instance but not the second. We

believe that our observations of conformers of different behavior for 1-naphthol$(NH_3)_3$ clusters help resolve the differences between the two previous[6,8] (dynamic and static) studies on this system. As shown in Figure 3, the feature at ca. 31,105 cm^{-1} for 1-naphthol$(NH_3)_3$ has a very small intensity which is mostly masked in the 1-color spectrum by high intensity species. Assuming that the transition probabilities for the $S_1 \leftarrow S_0$ and $I \leftarrow S_1$ steps of the neutral clusters are similar for these origin features, two explanations for the reduced intensity of the 31,105cm^{-1} feature are plausible: 1. the population of this conformer is low; and 2. the S_1 lifetime and the ionization cross section for this cluster are reduced due to the $AH^*(B_n) \rightarrow AH^{*-}(HB_n)^+$ proton transfer reaction. Both mechanisms are possible and may well contribute to the reduced intensity of this conformer of 1-naphthol$(NH_3)_3$. The unfortunate overlap between a strong 1-naphthol$(NH_3)_2$ and very weak 1-naphthol$(NH_3)_3$ probably explains why this feature has not been previously identified in dispersed emission proton transfer studies.[6] Of course, with picosecond time resolved studies, this 1-naphthol$(NH_3)_3$ conformer should be a dominant feature due to its greater concentration than $n \geq 4$ clusters and its time dependent mass detected signal.

C. Cluster Structure Calculations

Proton affinity of the solvent and stabilization (solvation) of the produced ions (A^{-*} and H^+) are two essential factors for the occurrence of excited state proton transfer reactions in clusters. The calculated cluster structures reported in the last section can aid in the understanding of the affect of solute/solvent geometry on the proton transfer reaction. While the calculations are certainly potential dependent and the one employed here is certainly arbitrary and surely only qualitative, the calculated trends are probably useful and indicative of the actual cluster behavior. Employing reasonable potentials should certainly generate cluster structures that embody the current state of knowledge of intermolecular interactions.

As shown in Figures 6 through 9, 1-naphthol$(H_2O)_n$ clusters achieve low energy structures that emphasize hydrogen bonding between all the molecules, especially the water molecules: the water molecules thus have a tendency (for the large binding energy cluster structures) to bind together and reside as a group in the vicinity of the 1-naphthol OH group. Therefore, the solvation of the naphthalene portion of the naphthol molecule tends to be poor and somewhat incomplete even for clusters with large amounts of solvent waters ($n > 5$).

The calculations suggest the opposite trend for 1-naphthol$(NH_3)_n$ clusters. Hydrogen bonding is much less emphasized for these clusters and the NH_3 - NH_3 interaction is small. Consequently, the ammonia molecules solvate both the OH and the aromatic moieties to a larger extent than found for the water solvent system even in small clusters. In addition, the probability for forming hydrogen bonded (O-H .... NH_3) structures seems to increase as the clusters become larger ($n = 3, 4$) in this system as suggested in Figures 11 and 12.

Thus, the experimental and calculational results seem to imply for these cluster systems the following characterization: 1. in 1-naphthol$(H_2O)_n$ the proton transfer reaction does not occur because the proton affinity of water is low and because the naphtholate anion is not well stabilized or solvated by the water; and 2. in 1-naphthol $(NH_3)_n$ clusters the solvation of both the proton and the naphtholate anion is good at relatively low solvent number ($n \sim 3$ to 4) and the ammonia proton affinity (although not necessarily hydrogen bonding preference or tendency) is relatively high. Cluster geometry and solvation structure at the margin of adequate solvation number seem to be essential features for the proton transfer reaction.

These above results are consistent with the time resolved matrice isolation studies of ref. 25 which find rapid (< 20 ps) proton transfer for 1-naphthol $(NH_3)_3$ clusters in an argon matrix.[25] Nonetheless, due to differences in solvation character, cluster structure, and Franck-Condon factors for absorption and proton transfer, the gas phase and matrix isolation cluster data need not be the same.

V. CONCLUSIONS

Based on threshold photo-ionization and dispersed emission data, we conclude that excited state proton transfer occurs in 1-naphthol/ammonia clusters for all $n \geq 4$ cluster conformations and (at least) one $n = 3$ cluster conformation. For all other ammonia and water clusters of 1-naphthol, no excited state proton transfer can be characterized. These results can be qualitatively rationalized on the basis of cluster structure and binding energy calculations. Calculations suggest that proton transfer is induced only if both proton and anion can be well solvated: for ammonia this occurs around $n = 3$ or 4 solvent molecules because ammonia has a reduced (with respect to water) specific hydrogen bonding interaction, a relatively weak NH_3 - NH_3 interaction, and an increased (with respect to water) cluster proton affinity.

REFERENCE

1. See papers in special issue for "Spectroscopy and Dynamics of Elementary Proton Transfer in Polyatomic Systems" in Chem. Phys. **136** (1989).
2. Atomic and Molecular Clusters, ed. E.R. Bernstein, (Elsevier, Amsterdam, 1990).
3. T. Förster, Z. Electrochem., **54**, 531 (1950).
4. J.F. Ireland and P.A. H. Wyatt, Adv. Phys. Org. Chem. **12**, 131 (1976).
5. O. Cheshnovsky and S. Leutwyler, Chem. Phys. Lett. **121**, 1 (1985).
6. O. Cheshnovsky and S. Leutwyler, J. Chem. Phys. **88**, 4127 (1988).
7. R. Knochenmuss, O. Cheshnovsky and S. Leutwyler, Chem. Phys. Lett. **144**, 317 (1988).
8. J.J. Breen, L.W. Peng, D.M. Willberg, A. Heikal, P. Cong and A.H. Zewail, J. Chem. Phys. **92**, 805 (1990).
9. T. Dorz, R. Knochenmuss and S. Lewtwyler, J. Chem. Phys. **93**, 4520 (1990).
10. D. Solgadi, C. Jouvet and A. Tramer, J. Phys. Chem. **92**, 3313 (1988).
11. J. Steadman and J.A. Syage, J. Chem. Phys. **92**, 4630 (1990).
12. C. Jouvet, C. Lardeux-Dedonder, M. Richard-Viard, D. Solgadi and A. Tramer, J. Phys. Chem. **94**, 5041 (1990).
13. M.R. Nimlos, D.F. Kelley and E.R. Bernstein, J. Phys. Chem. **93**, 643 (1989).
14. N.P. Ernsting, J. Phys. Chem. **89**, 4932 (1985).
    N.P. Ernsting, J. Am. Chem. Soc. **107**, 4564 (1985).
15. S. K. Kim, S.-C. Hsu and E.R. Bernstein in preparation.
16. N. Mikami, I. Suzuki and A. Okabe, J. Phys. Chem. **91**, 5242 (1987).
17. R. Knochenmuss and S. Leutwyler, J. Chem. Phys. **91**, 1268 (1989).
18. E.R. Bernstein, K. Law and M. Schauer, J. Chem. Phys. **80**, 207 (1984).
19. G. Nemethy, M.S. Pottle and H.A. Scherga, J. Phys. Chem, **87**, 188 (1983).
    F.A. Momany, L.M. Carruthers, R.F. McGuire and H.A. Scherga, J. Phys. Chem. **78**, 1595 (1974).

20. J.J.P. Stewart, J. Comput. Chem. **10**, 209, 221 (1989).

21. J. M. Hollas and M.Z.B. Hussein, J. Mol. Spec. **127**, 497 (1988).

22. C. Lakshminarayan and J.L. Knee, J. Phys. Chem. **94**, 2637 (1990).

23. J. R. Johnson, K. D. Jordan, D. F. Plusquellic, D. W. Pratt, J. Chem. Phys **93**, 2258 (1990).

24. J. Hager, M. Ivanco, M.A. Smith and S.C. Wallace, Chem. Phys. **105**, 397 (1986).

25. G. A. Brucker, D. F. Kelley, J. Chem. Phys. **90**, 5243 (1989) and Chem. Phys. **136**, 213 (1989).

Table I

Summary of threshold photo-ionization for 1-naphthol and its NH_3 and H_2O clusters.

Sample	Excitation Frequency (ν_{ex}, cm^{-1})	$S_1 \rightarrow I$ Threshold (ν_{ion}, cm^{-1})	Ionization Potential (I.P.) ($\nu_{ex}+\nu_{ion}$, cm^{-1})	Shift of I.P. from bare molecular I.P. (cm^{-1})
1-naphthol	31458	31130±3	62588±3	0
1-naphthol$(H_2O)_1$	31310	27680±50	58990±50	-3598
1-naphthol$(NH_3)_1$	31221	26420±50	57641±50	-4947
1-naphthol$(NH_3)_2$	31105	26460±50	57525±50	-5063
1-naphthol$(NH_3)_3$	31047	26350±80	57397±80	-5191
"	31068	> 26420	> 57488	> -5100
"	31105	24840±50	55944±50	-6644
1-naphthol$(NH_3)_4$	30877	24990±50	55867±50	-6721
1-naphthol$(NH_3)_5$	30877	<24520	<55408	<-7180

Figure Captions:

Figure 1 a: The expected potential curves for the excited state proton transfer in $(AH)B_n$ systems. In this example, n=3 is the critical number of B solvent molecules for proton transfer. The symbols ν_{em} and ν'_{em} stand for the normal and proton transfer emission, respectively, and ν_1 and ν_2 are the normal and proton transfer $I \leftarrow S_1$ transition energies, respectively. ν_{ex} is the normal excitation $S_1 \leftarrow S_o$ energy.

b: The expected threshold photo-ionization spectra for the corresponding system. The suceesive red-shifts in the ionization thresholds upon additional clustering are due to the binding energy increases in the ionization state. Much larger red-shift in the ionization threshold is expected for n=3 due to the separation of the charges in the product. The ionization transitions ν_1 and ν_2 are indicated for n=3.

Figure 2: 1-color TOFMS of 1-naphthol and its clusters with H_2O and NH_3. Some possible fragmentation peaks are marked with *.

Figure 3 a: 1-color TOFMS of 1-naphthol$(NH_3)_3$.

b: 2-color TOFMS of 1-naphthol$(NH_3)_3$. The ionization laser energy is 26,420 cm^{-1}.

Figure 4: The threshold photo-ionization spectra of 1-naphthol clusters. □: 1-naphthol$(NH_3)_1$ (ν_{ex}= 31,221 cm^{-1}); ■: 1-naphthol$(NH_3)_2$ (ν_{ex}= 31,105 cm^{-1}); +: 1-naphthol$(NH_3)_3$ (ν_{ex}= 31,105 cm^{-1}); ○: 1-naphthol$(NH_3)_4$ (ν_{ex}= 30,877 cm^{-1}); Δ: 1-naphthol$(H_2O)_1$ (ν_{ex}= 31,310 cm^{-1}). Excitations at 31,068 cm^{-1}, 31,077 cm^{-1}, 31,080 cm^{-1}, 31,088 cm^{-1} for other conformers of 1-naphthol$(NH_3)_3$ have the similar threshold photo-ionization behavior to 1-naphthol$(NH_3)_{1,2}$. Threshold photo-ionization of 1-naphthol$(H_2O)_{2,3,4}$ are similar to 1-naphthol$(H_2O)_1$.

Figure 5 : Fluorescence excitation spectra for 1-naphthol/NH_3 with a UV34 filter (a), a UV36 filter (b), a L38 filter (c). 0.002% NH_3 in helium is used for expansion. Transmissions of the filters are the following: UV34 (0% < 315 nm, 2.5% at 320 nm, 52% at 340 nm, 80% at 360 nm, 84% at 380 nm, 87% > 400 nm); UV36

(0% < 340 nm, 47% at 360 nm, 74% at 380 nm, 83% at 400 nm, 86% > 440 nm); L38 (0% < 355 nm, 47% at 380 nm, 78% at 400 nm, 86% at 420 nm, 90% > 460 nm).

Figure 6: Calculated geometries for 1-naphthol$(H_2O)_1$. The stabilization energy and the percentage of the total number of calculations resulting in the reported structure are indicated.

Figure 7: The three most stable geometries for 1-naphthol$(H_2O)_2$. The stabilization energy and the percentage of the total number of calculations resulting in the reported structure are indicated.

Figure 8: The four most stable geometries for 1-naphthol$(H_2O)_3$. The stabilization energy and the percentage of the total number of calculations resulting in the reported structure are indicated.

Figure 9: The four most stable geometries for 1-naphthol$(H_2O)_4$. The geometry in (d) is calculated with one of H_2O molecule forced to make hydrogen bonding. The stabilization energy and the percentage of the total number of calculations resulting in the structure are indicated.

Figure 10(a), (b): The two most stable geometries for 1-naphthol$(NH_3)_1$. The geometry in (c) is achieved only if the starting geometry is chosen to favor hydrogen bonding. The stabilization energy and the percentage of the total number of calculations resulting in the reported structure are indicated.

Figure 11(a), (b): The two most stable geometries for 1-naphthol$(NH_3)_2$. The geometry in (c) is calculated only if one NH_3 is forced into a hydrogen bonding structure. The stabilization energy and the percentage of the total number of calculations resulting in the reported structure are indicated.

Figure 12(a), (b), (c): The three most stable geometries for 1-naphthol$(NH_3)_3$. The geometry in (d) is calculated only if one NH_3 is forced into a hydrogen bonding structure. The stabilization energy and the percentage of the total number of calculations resulting in the reported structure are indicated.

Figure 13(a), (b), (c): The three most stable geometries for 1-naphthol$(NH_3)_4$. The geometry in (d) is calculated only if one NH_3 is forced into a hydrogen bonding structure. The stabilization energy and the percentage of the total number of calculations resulting in the reported structure are indicated.

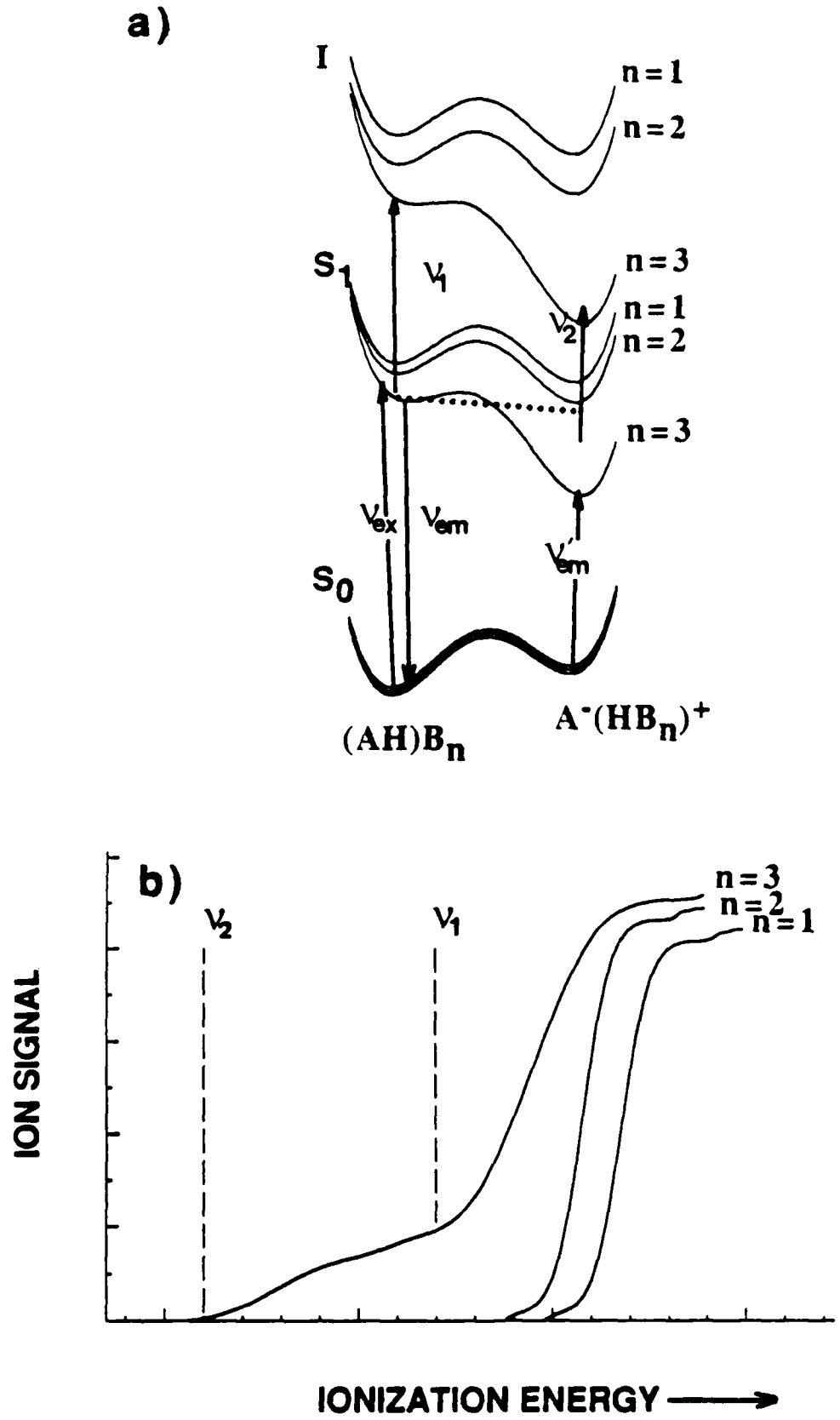
a)
I
n=1
n=2
S1
ν1
n=3
n=1
ν2
n=2
n=3
νex
νem
ν'em
S0
(AH)Bn
A-(HBn)+
b)
ν2
ν1
n=3
n=2
n=1
ION SIGNAL
IONIZATION ENERGY ⟶

Fig. 1

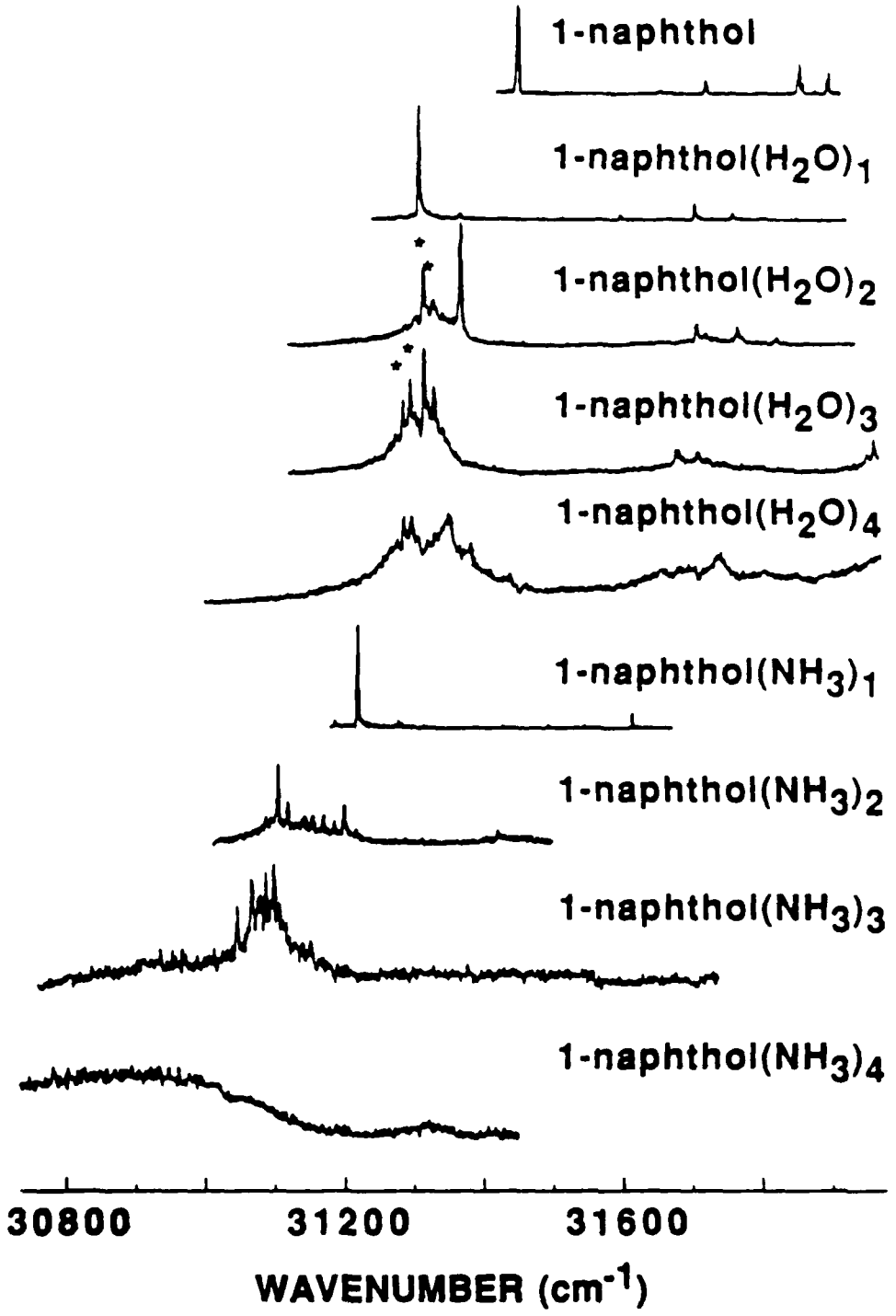
1-naphthol
1-naphthol(H2O)1
1-naphthol(H2O)2
1-naphthol(H2O)3
1-naphthol(H2O)4
1-naphthol(NH3)1
1-naphthol(NH3)2
1-naphthol(NH3)3
1-naphthol(NH3)4
30800
31200
31600
WAVENUMBER (cm-1)

Fig. 2

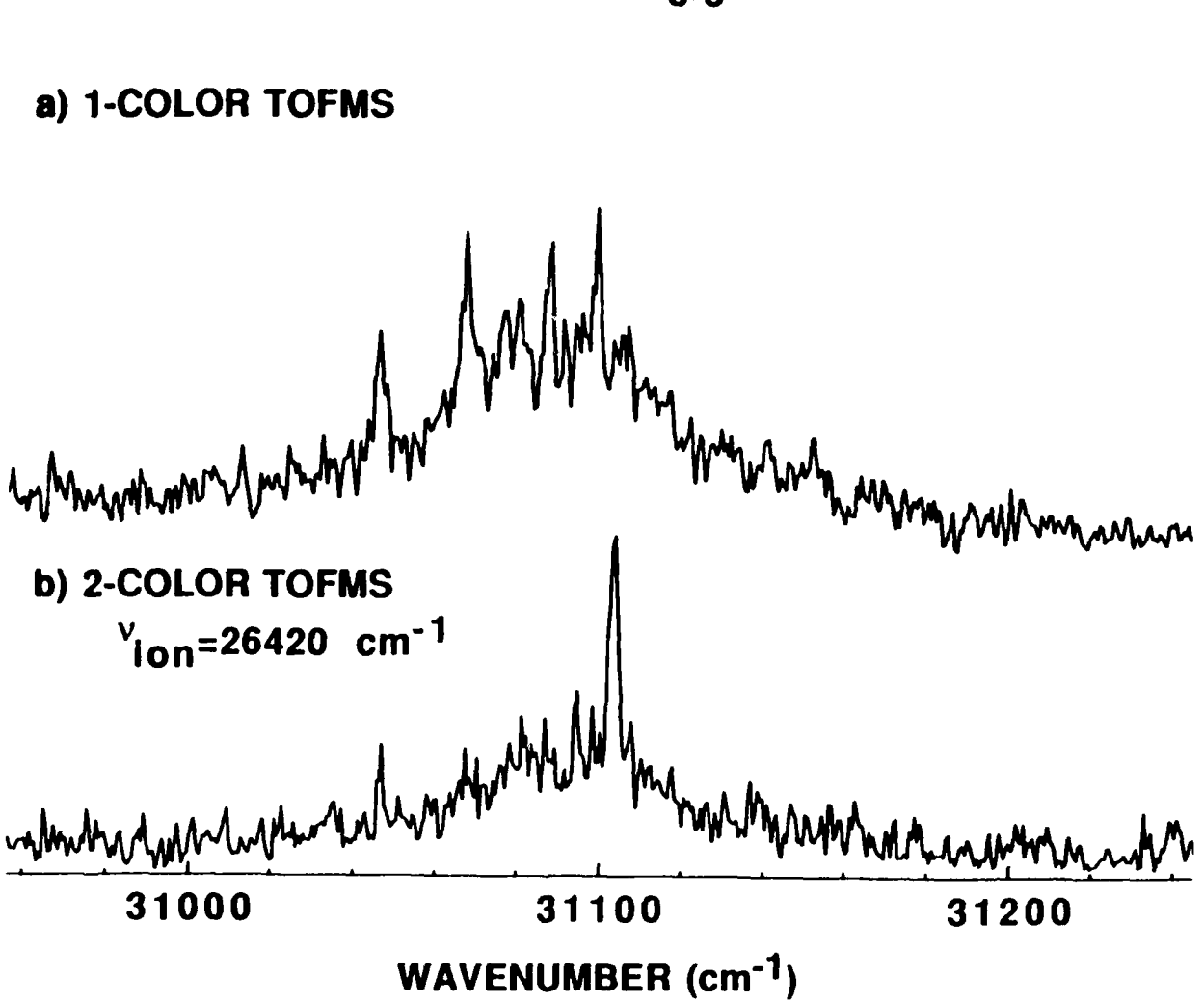
1-naphthol(NH3)3
a) 1-COLOR TOFMS
b) 2-COLOR TOFMS
νion=26420 cm-1
31000
31100
31200
WAVENUMBER (cm-1)

Fig. 3

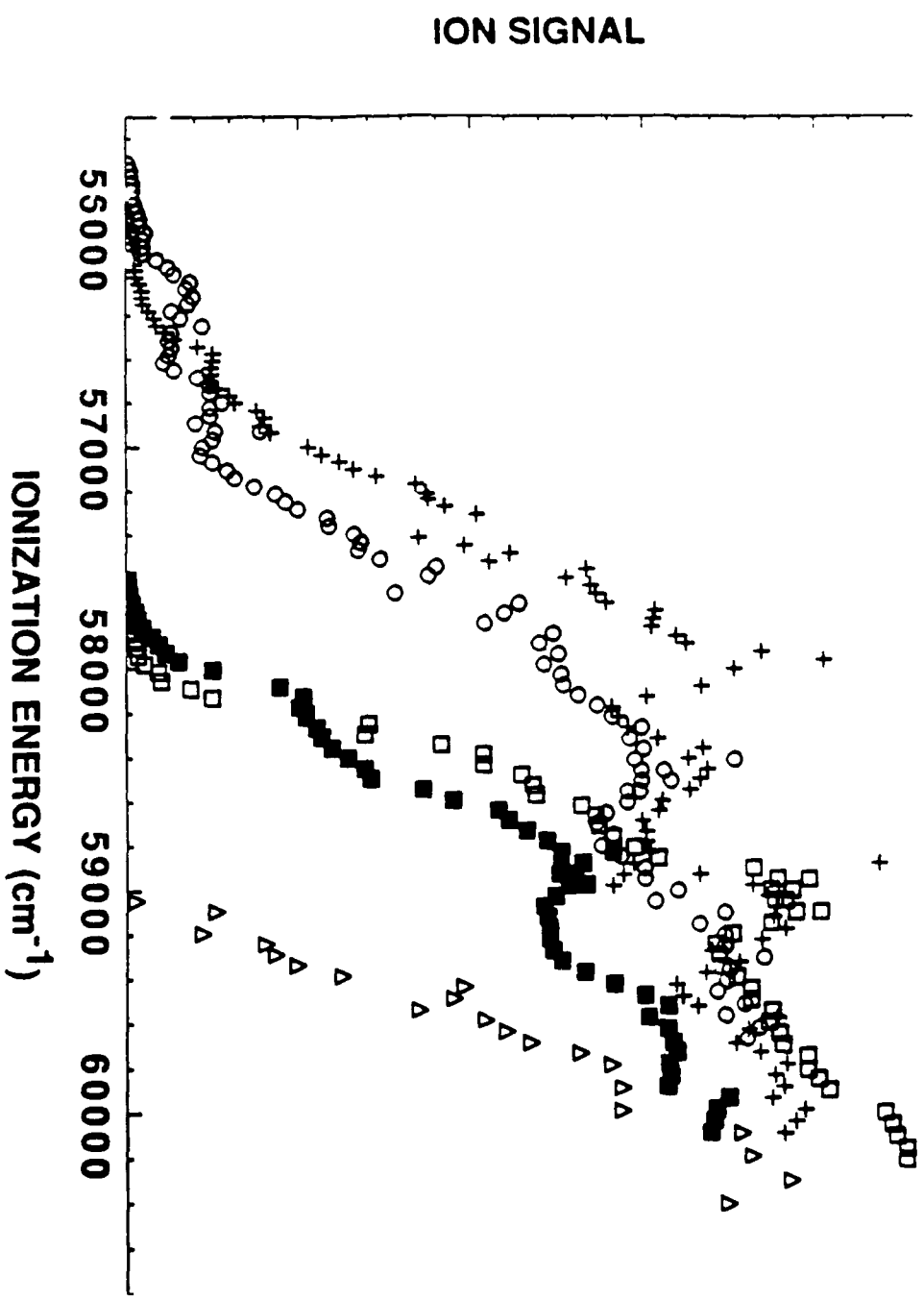
ION SIGNAL
IONIZATION ENERGY (cm-1)
55000
57000
58000
59000
60000

Fig. 4

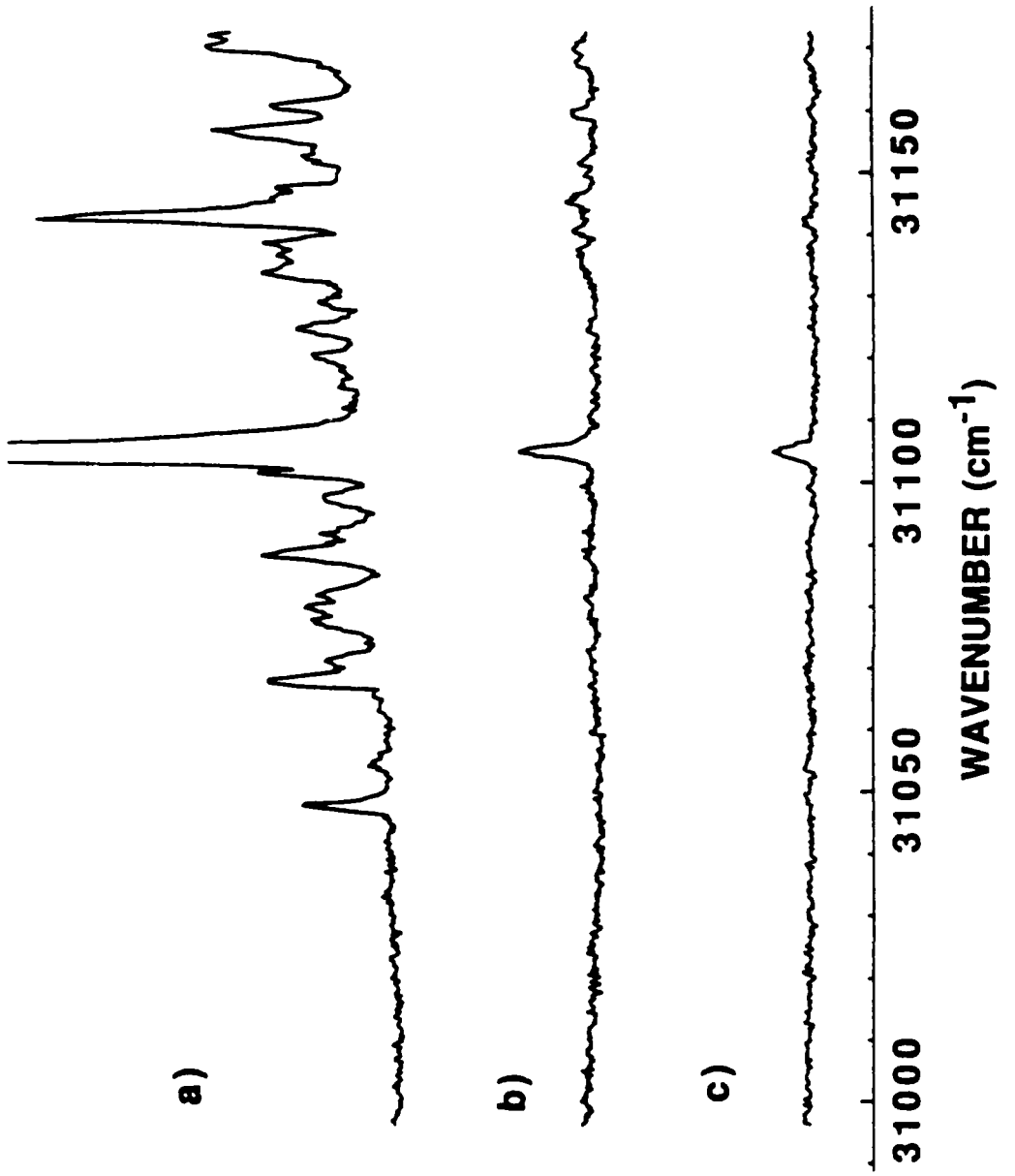

Fig. 5

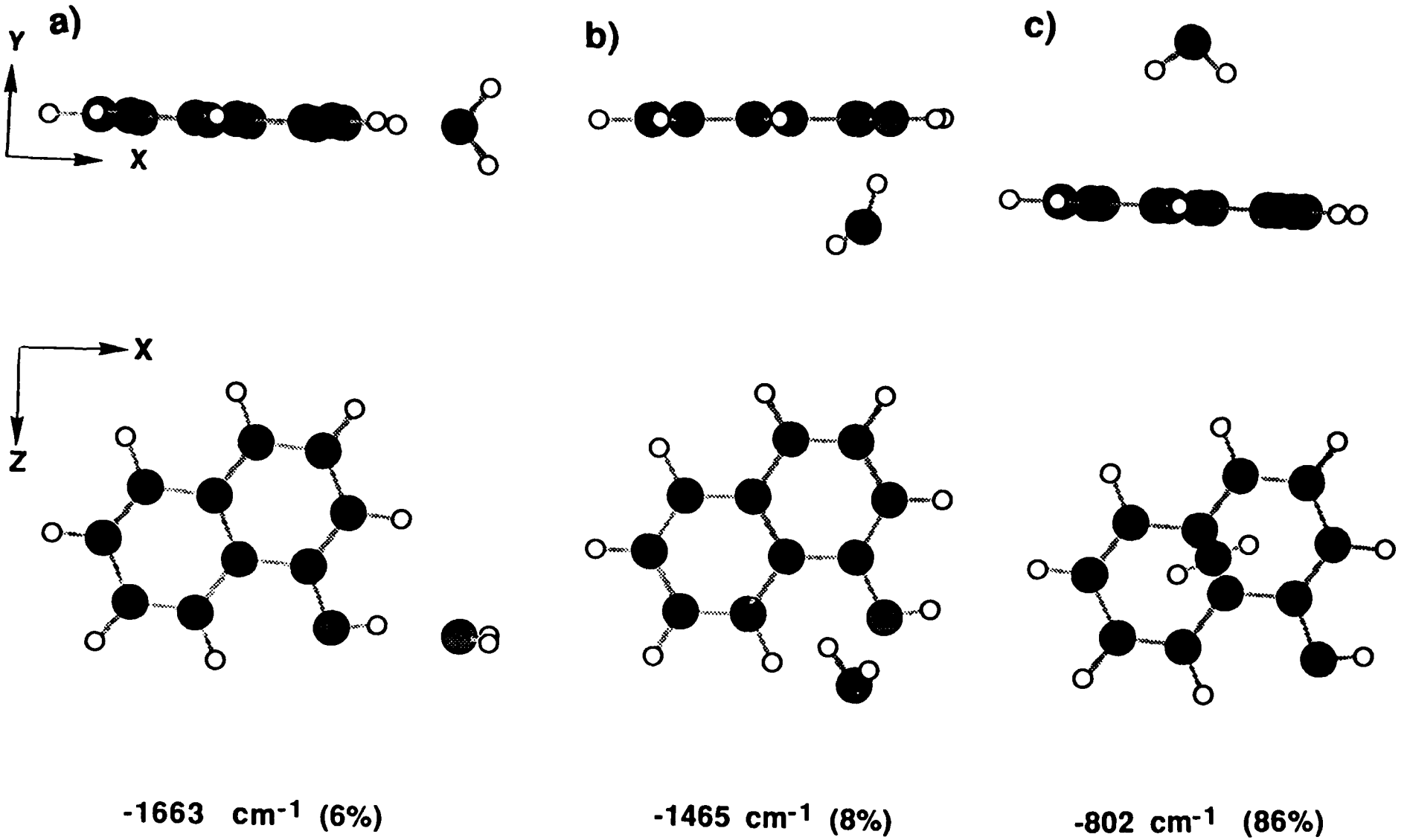

Fig. 6

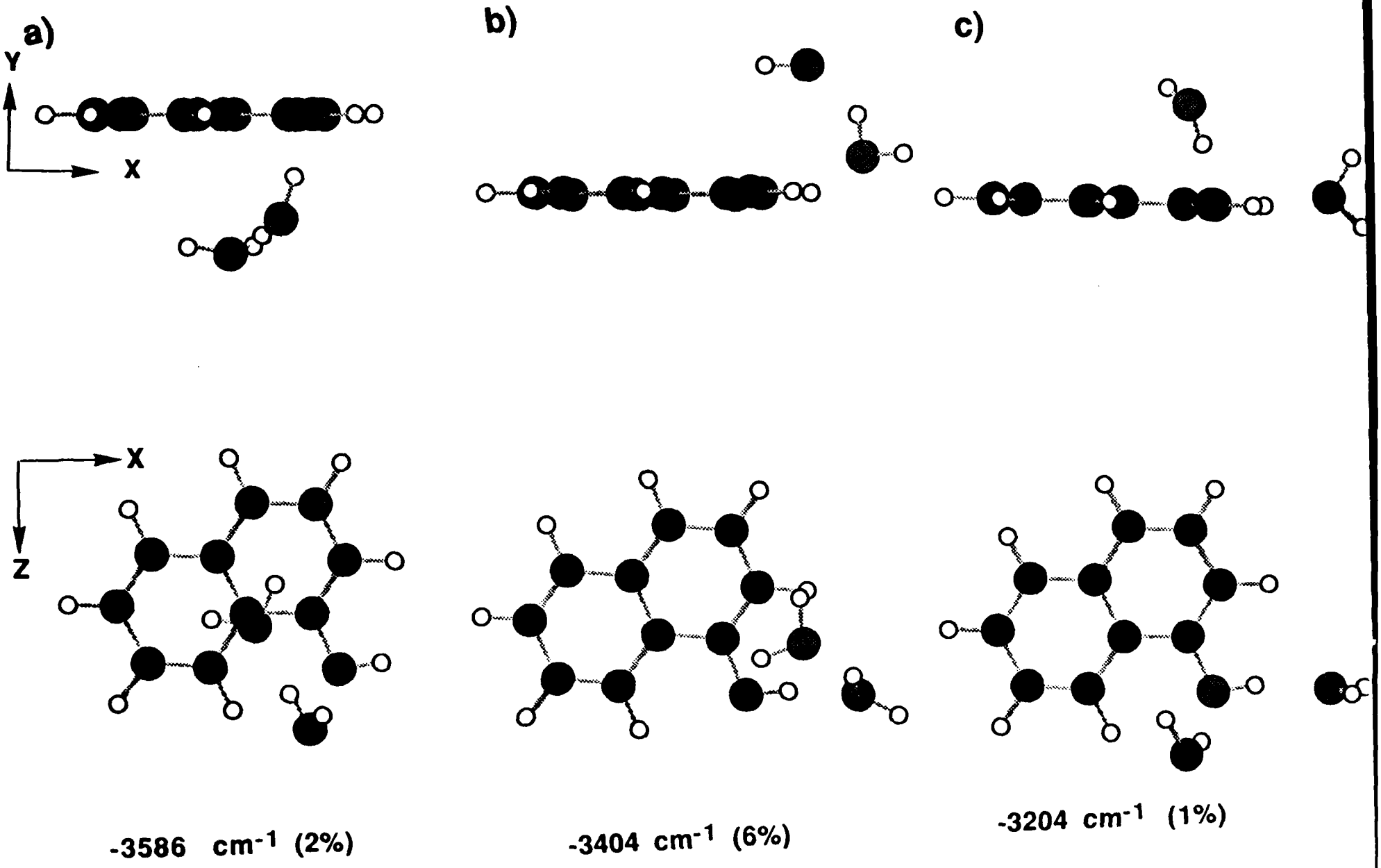

Fig. 7

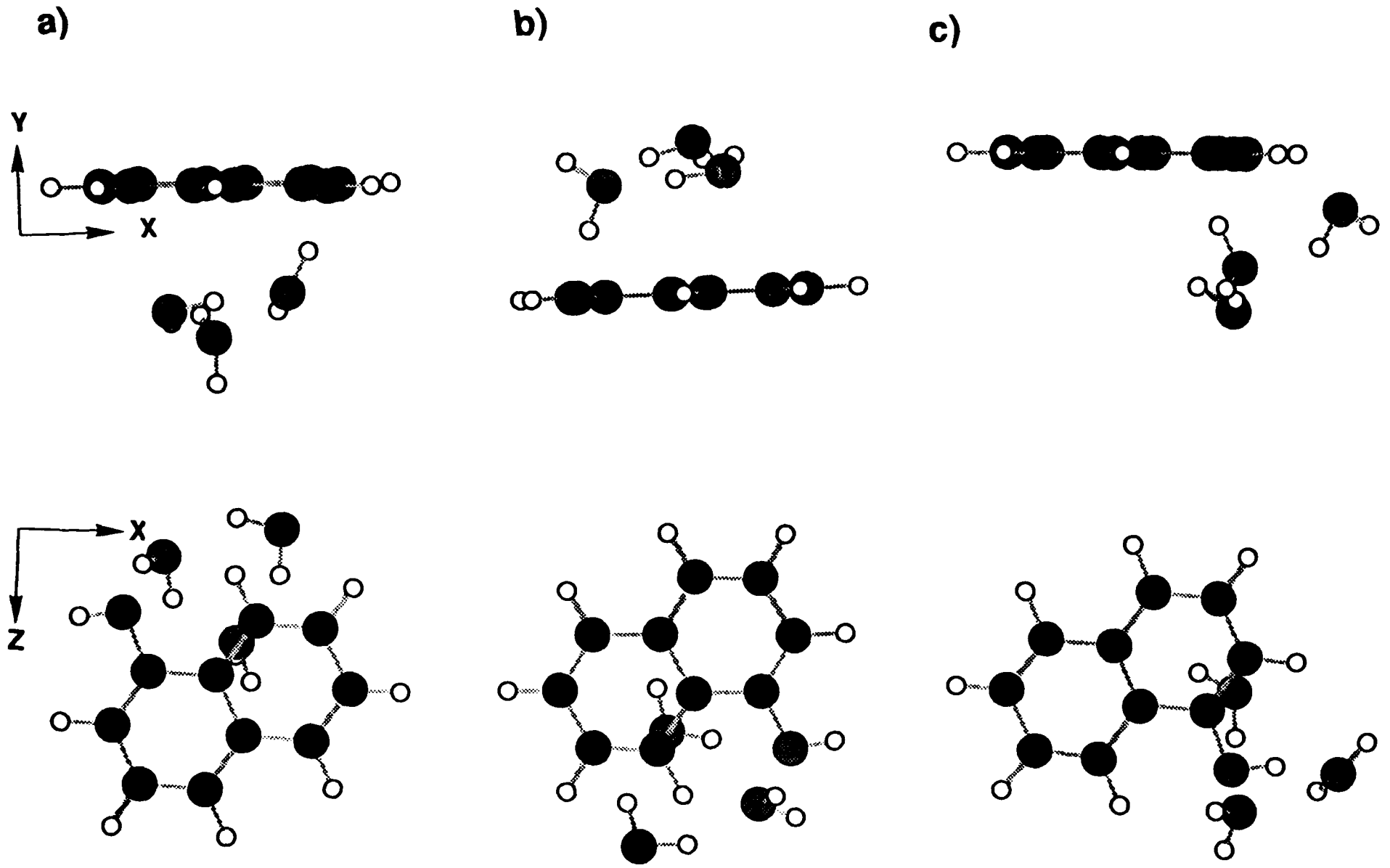

Fig. 8

d)

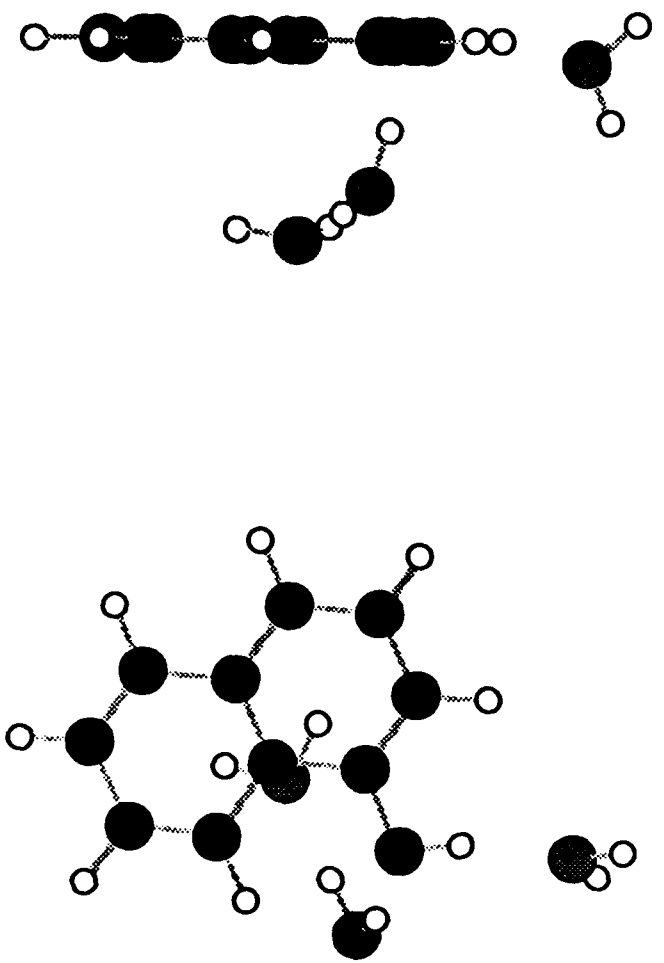

-5326 cm^{-1} (2%)

Fig. 8

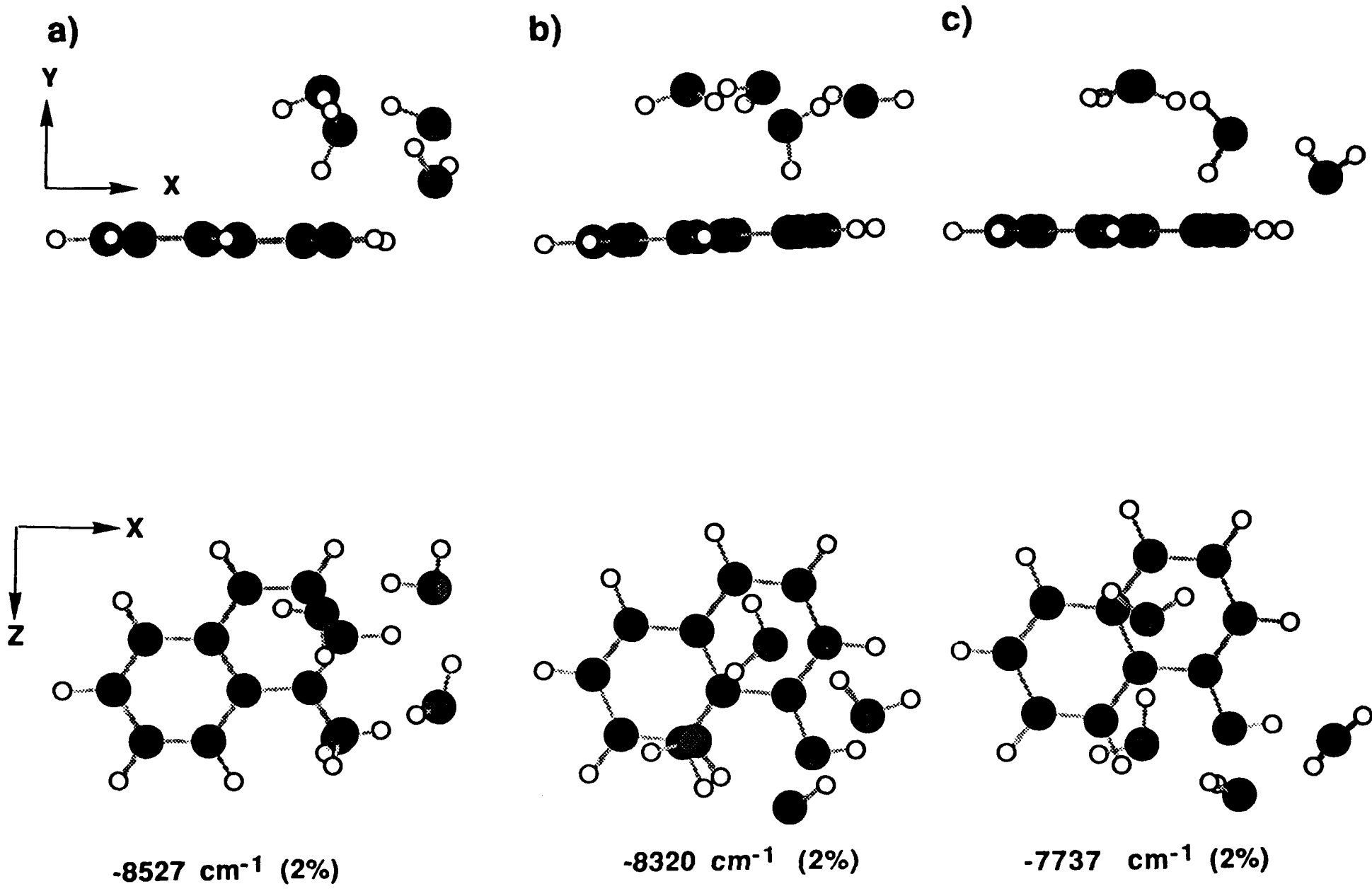

Fig. 9

Fig. 9

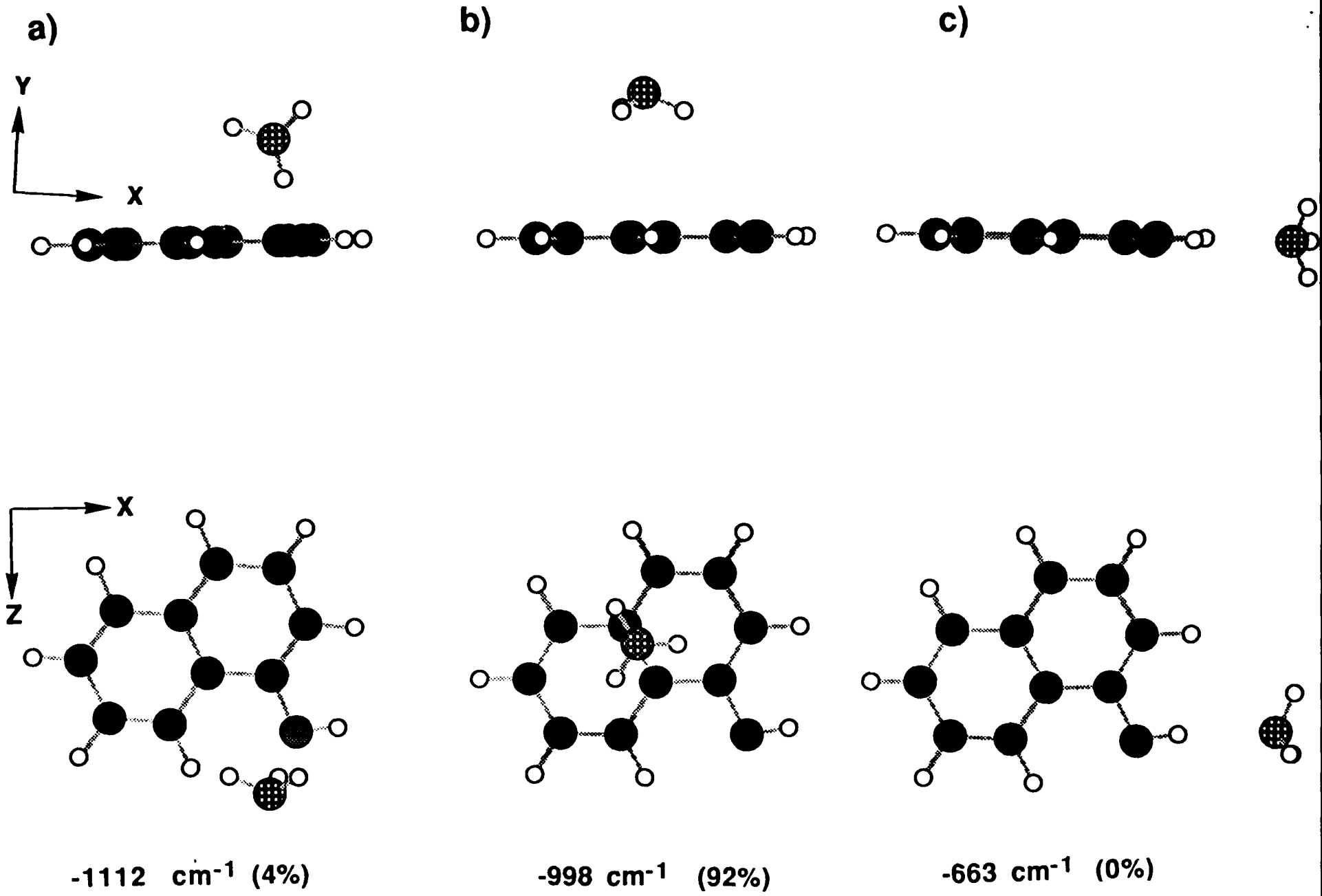

Fig. 10

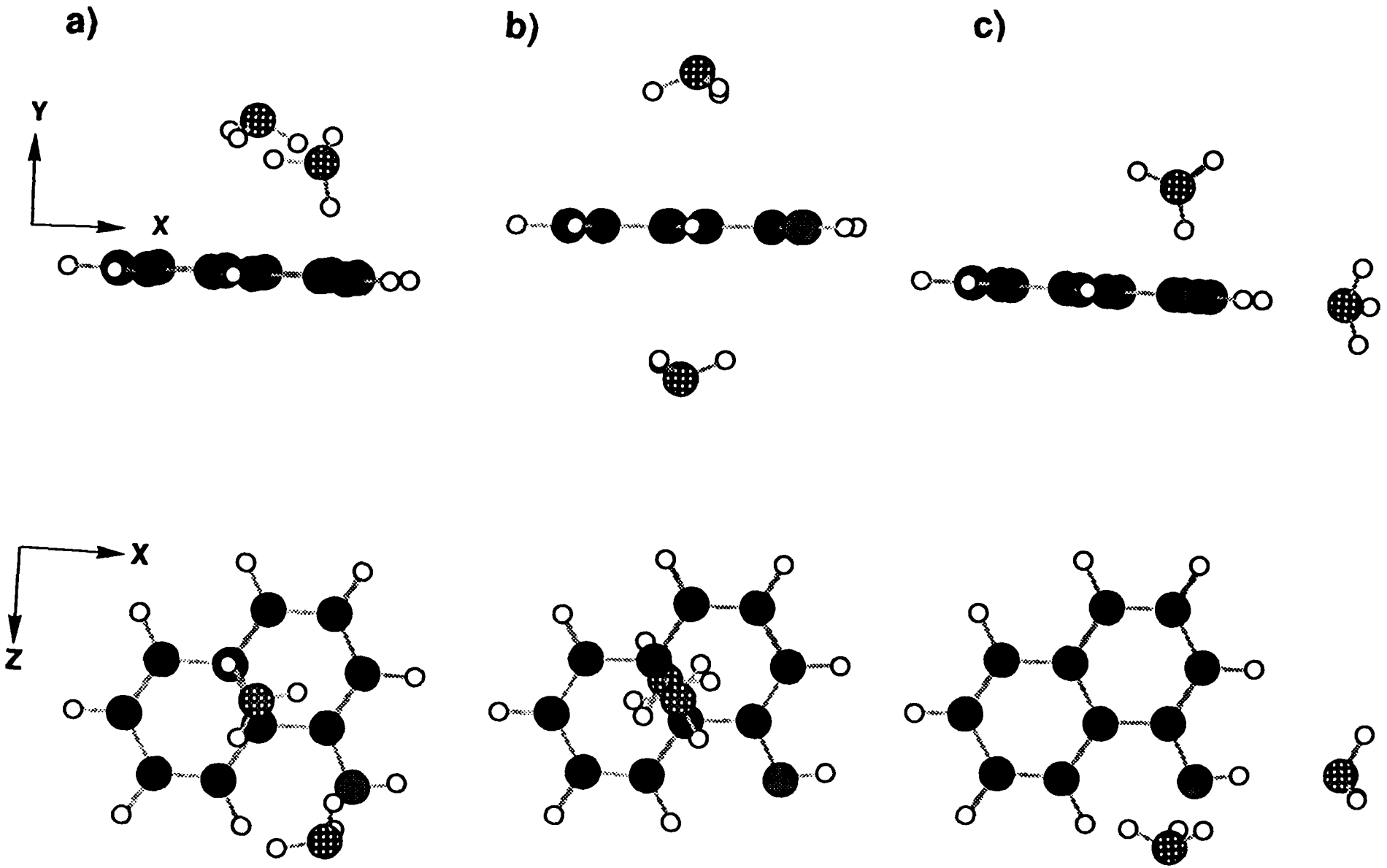

Fig. 11

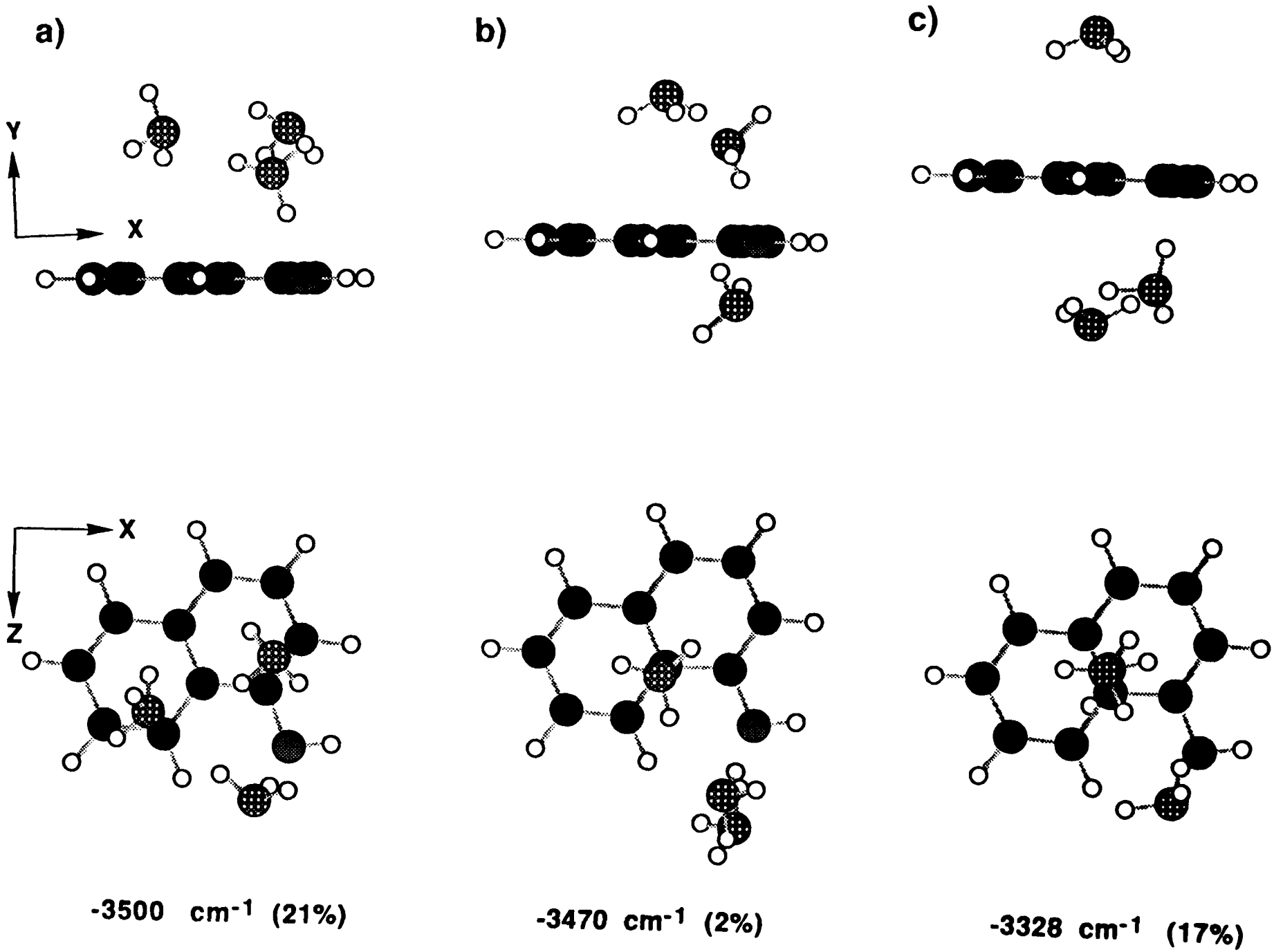

Fig. 12

d)

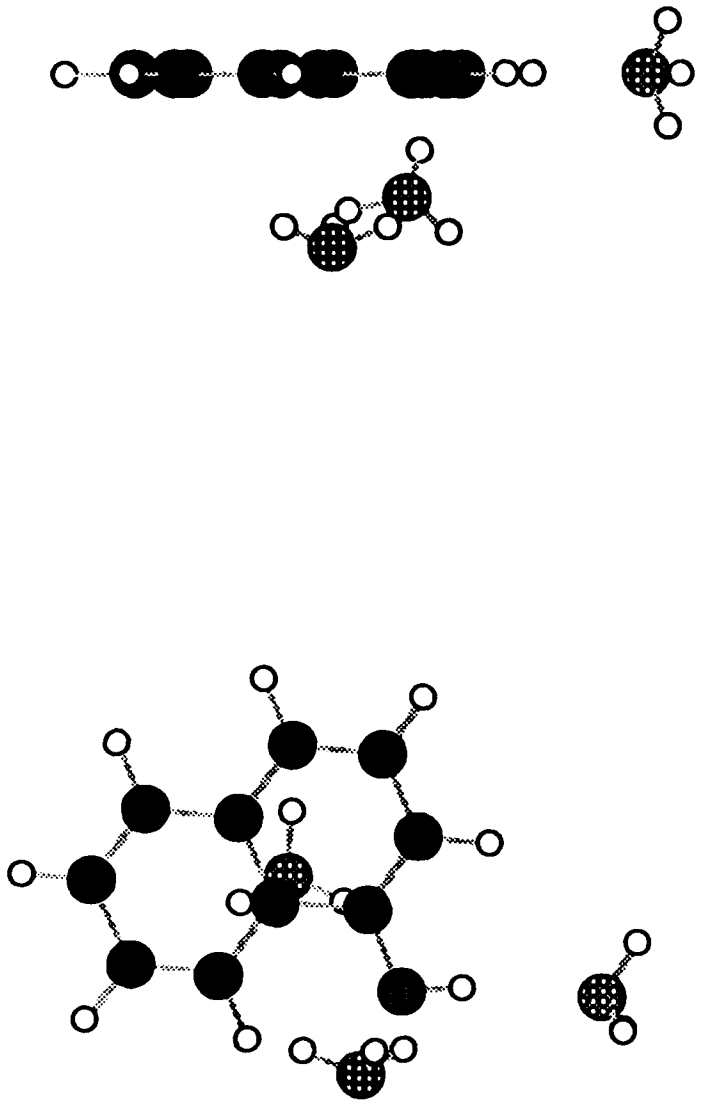

-3038 cm^{-1} (0%)

Fig. 12

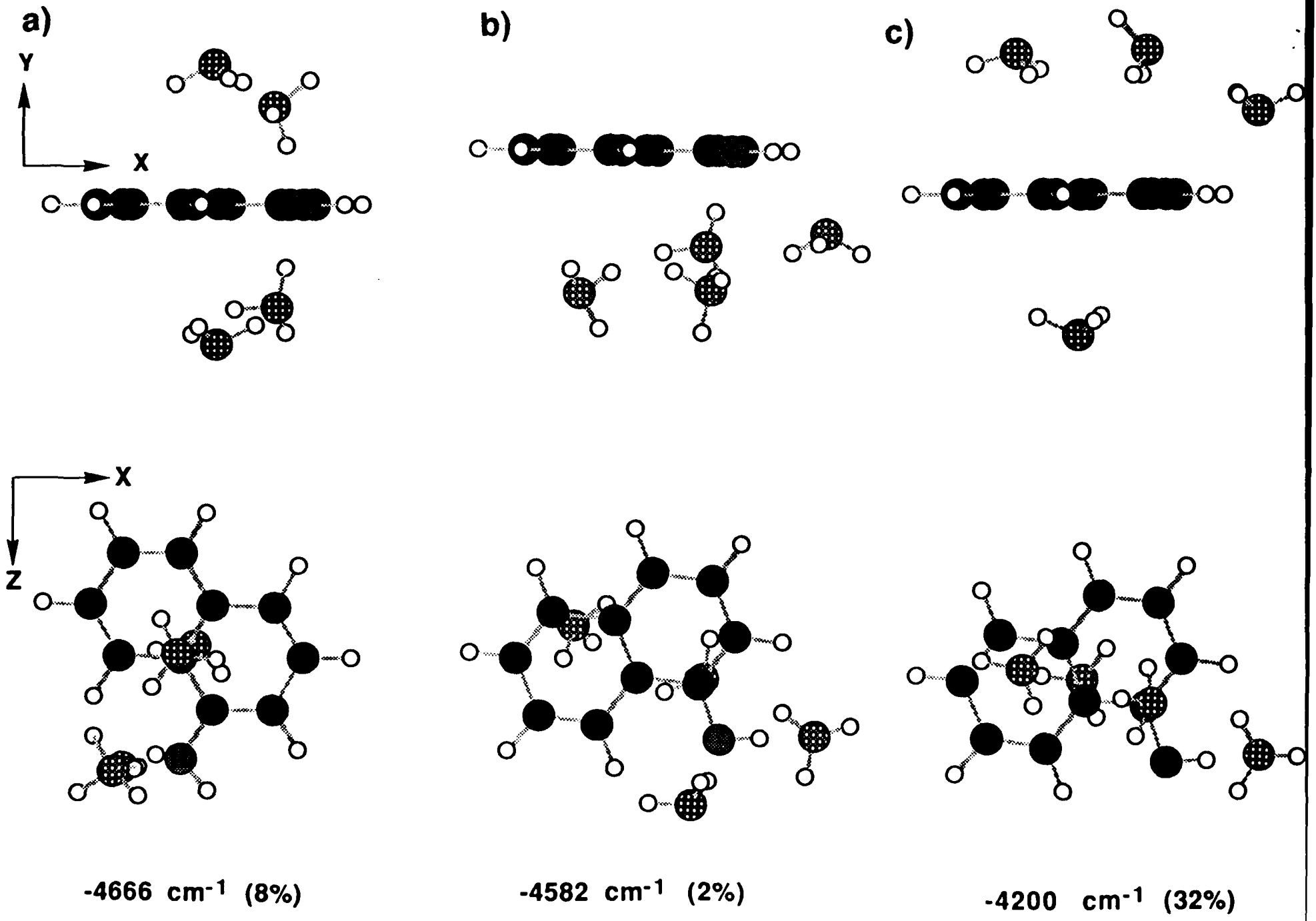

Fig. 13

Fig. 13